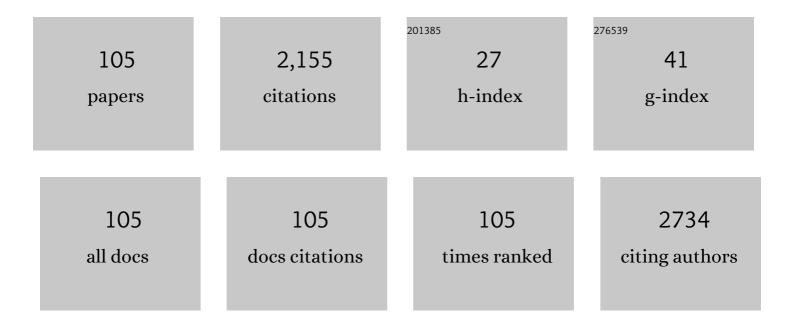
List of Publications by Year in descending order

Source: https://exaly.com/author-pdf/5121999/publications.pdf Version: 2024-02-01



#	Article	IF	CITATIONS
1	Intraductal Papillary Mucinous Neoplasm of the Pancreas: Assessment of the Likelihood of Invasiveness with Multisection CT. Radiology, 2008, 248, 876-886.	3.6	105
2	Diffusion-Weighted Imaging of Breast Masses: Comparison of Diagnostic Performance Using Various Apparent Diffusion Coefficient Parameters. American Journal of Roentgenology, 2012, 198, 717-722.	1.0	92
3	Assessment of the pancreatic and intrapancreatic bile ducts using 0.5-mm collimation and multiplanar reformatted images in multislice CT. European Radiology, 2003, 13, 277-285.	2.3	75
4	Evaluation and comparison of 11C-choline uptake and calcification in aortic and common carotid arterial walls with combined PET/CT. European Journal of Nuclear Medicine and Molecular Imaging, 2009, 36, 1622-1628.	3.3	73
5	Comparison of 18F-FDG PET and Bone Scintigraphy in Detection of Bone Metastases of Thyroid Cancer. Journal of Nuclear Medicine, 2007, 48, 889-895.	2.8	68
6	Fluorodeoxyglucose positron emission tomography in pancreatic cancer: an unsolved problem. European Journal of Nuclear Medicine and Molecular Imaging, 1995, 22, 32-39.	2.2	66
7	A scintigraphical qualitative analysis of peripheral vascular sympathetic function with meta-[1231]iodobenzylguanidine in neurological patients with autonomic failure. Journal of the Autonomic Nervous System, 1995, 53, 230-234.	1.9	66
8	Diagnostic value of curved multiplanar reformatted images in multislice CT for the detection of resectable pancreatic ductal adenocarcinoma. European Radiology, 2006, 16, 1709-1718.	2.3	63
9	Comparison of Contrast Effect on the Cochlear Perilymph after Intratympanic and Intravenous Gadolinium Injection. American Journal of Neuroradiology, 2012, 33, 773-778.	1.2	63
10	Lung nodule detection performance in five observers on computed tomography (CT) with adaptive iterative dose reduction using three-dimensional processing (AIDR 3D) in a Japanese multicenter study: Comparison between ultra-low-dose CT and low-dose CT by receiver-operating characteristic analysis. European Journal of Radiology, 2015, 84, 1401-1412.	1.2	59
11	Semi-quantification of Endolymphatic Size on MR Imaging after Intravenous Injection of Single-dose Gadodiamide: Comparison between Two Types of Processing Strategies. Magnetic Resonance in Medical Sciences, 2013, 12, 261-269.	1.1	57
12	Differentiation of focal-type autoimmune pancreatitis from pancreatic carcinoma: assessment by multiphase contrast-enhanced CT. European Radiology, 2015, 25, 1366-1374.	2.3	56
13	Prospective Analysis of Mortality, Morbidity, and Risk Factors in Elderly Diabetic Subjects: Nagano Study. Diabetes Care, 2003, 26, 638-644.	4.3	53
14	Late-arterial and portal-venous phase imaging of the liver with a multislice CT scanner in patients without circulatory disturbances: automatic bolus tracking or empirical scan delay?. European Radiology, 2004, 14, 1665-73.	2.3	47
15	Relationship between CT densitometry with a slice thickness of 0.5Âmm and audiometry in otosclerosis. European Radiology, 2006, 16, 1367-1373.	2.3	46
16	Predictive Value for Malignancy of Suspicious Breast Masses of BI-RADS Categories 4 and 5 Using Ultrasound Elastography and MR Diffusion-Weighted Imaging. American Journal of Roentgenology, 2011, 196, 202-209.	1.0	46
17	Prediction of Outcomes in Mild Cognitive Impairment by Using 18F-FDG-PET: A Multicenter Study. Journal of Alzheimer's Disease, 2015, 45, 543-552.	1.2	44
18	Endolympathic hydrops in patients with vestibular schwannoma: visualization by non-contrast-enhanced 3D FLAIR. Neuroradiology, 2011, 53, 1009-1015.	1.1	43

#	Article	IF	CITATIONS
19	Computer-aided differentiation of malignant from benign solitary pulmonary nodules imaged by high-resolution CT. Computerized Medical Imaging and Graphics, 2008, 32, 416-422.	3.5	40
20	Fluorine-18 fluoro-2-deoxyglucose positron emission tomography in recurrent rectal cancer: relation to tumour size and cellularity. European Journal of Nuclear Medicine and Molecular Imaging, 1996, 23, 1372-1377.	2.2	39
21	Limited Efficacy of 18F-FDG PET/CT for Differentiation Between Metastasis-Free Pancreatic Cancer and Mass-Forming Pancreatitis. Clinical Nuclear Medicine, 2013, 38, 417-421.	0.7	38
22	Correlation between Estimated Glomerular Filtration Rate (eGFR) and Apparent Diffusion Coefficient (ADC) Values of the Kidneys. Magnetic Resonance in Medical Sciences, 2010, 9, 59-64.	1.1	35
23	Statistical characteristics of streak artifacts on CT images: Relationship between streak artifacts and mA s values. Medical Physics, 2009, 36, 492-499.	1.6	34
24	Multiphase contrast-enhanced CT of the liver with a multislice CT scanner. European Radiology, 2003, 13, 1085-1094.	2.3	32
25	Cerebral glucose metabolism change in patients with complex regional pain syndrome: a PET study. Radiation Medicine, 2006, 24, 335-344.	0.8	32
26	Interactions of perceptual and conceptual processing: Expertise in medical image diagnosis. International Journal of Human Computer Studies, 2008, 66, 370-390.	3.7	32
27	Branch duct-type intraductal papillary mucinous tumor: diagnostic value of multiplanar reformatted images in multislice CT. European Radiology, 2005, 15, 1888-1897.	2.3	29
28	Relationship between Brier score and area under the binormal ROC curve. Computer Methods and Programs in Biomedicine, 2002, 67, 187-194.	2.6	27
29	Parieto-occipital glucose hypometabolism in Parkinson's disease with autonomic failure. Journal of the Neurological Sciences, 1999, 163, 119-126.	0.3	26
30	Time Course for Measuring Endolymphatic Size in Healthy Volunteers Following Intravenous Administration of Gadoteridol. Magnetic Resonance in Medical Sciences, 2014, 13, 73-80.	1.1	26
31	A Randomized, Double-Blind Pilot Trial of Hydrolyzed Rice Bran versus Placebo for Radioprotective Effect on Acute Gastroenteritis Secondary to Chemoradiotherapy in Patients with Cervical Cancer. Evidence-based Complementary and Alternative Medicine, 2015, 2015, 1-6.	0.5	23
32	Influence of CRT workstation on observer's performance. Computer Methods and Programs in Biomedicine, 1992, 37, 253-258.	2.6	21
33	Evaluation of a neural network classifier for pancreatic masses based on CT findings. Computerized Medical Imaging and Graphics, 1997, 21, 175-183.	3.5	21
34	Establishing Normal Diameter Range of the Cochlear and Facial Nerves with 3D-CISS at 3T. Magnetic Resonance in Medical Sciences, 2013, 12, 241-247.	1.1	21
35	Maximal calf circumference reflects calf muscle mass measured using magnetic resonance imaging. Archives of Gerontology and Geriatrics, 2019, 83, 175-178.	1.4	21
36	Evaluation of 11C-choline PET/CT for primary diagnosis and staging of urothelial carcinoma of the upper urinary tract: a pilot study. European Journal of Nuclear Medicine and Molecular Imaging, 2014, 41, 2232-2241.	3.3	19

#	Article	IF	CITATIONS
37	Ratio of Vestibular Endolymph in Patients with Isolated Lateral Semicircular Canal Dysplasia. Magnetic Resonance in Medical Sciences, 2015, 14, 203-210.	1.1	19
38	The Effect of Patient Age on Contrast Enhancement During CT of the Pancreatobiliary Region. American Journal of Roentgenology, 2006, 187, 505-510.	1.0	18
39	Heavily T ₂ -Weighted 3D-FLAIR Improves the Detection of Cochlear Lymph Fluid Signal Abnormalities in Patients with Sudden Sensorineural Hearing Loss. Magnetic Resonance in Medical Sciences, 2016, 15, 203-211.	1.1	18
40	Lung: Feasibility of a Method for Changing Tube Current during Low-Dose Helical CT. Radiology, 2002, 224, 905-912.	3.6	17
41	Solitary pulmonary nodules. Clinical Imaging, 2004, 28, 322-328.	0.8	17
42	Comparison of Liquid Crystal Display Monitors Calibrated With Gray-Scale Standard Display Function and With γ 2.2 and iPad: Observer Performance in Detection of Cerebral Infarction on Brain CT. American Journal of Roentgenology, 2013, 200, 1304-1309.	1.0	16
43	Quantitative assessment of image noise and streak artifact on CT image: Comparison of z-axis automatic tube current modulation technique with fixed tube current technique. Computerized Medical Imaging and Graphics, 2009, 33, 353-358.	3.5	15
44	Volume Quantification of Endolymph after Intravenous Administration of a Single Dose of Gadolinium Contrast Agent: Comparison of 18- versus 8-minute Imaging Protocols. Magnetic Resonance in Medical Sciences, 2015, 14, 257-262.	1.1	15
45	A method for estimating noise variance of CT image. Computerized Medical Imaging and Graphics, 2010, 34, 642-650.	3.5	14
46	Arterial contour detectability in head CT angiography. International Journal of Computer Assisted Radiology and Surgery, 2015, 10, 1-10.	1.7	14
47	Cochlear Lymph Fluid Signal Increase in Patients with Otosclerosis after Intravenous Administration of Gadodiamide. Magnetic Resonance in Medical Sciences, 2016, 15, 308-315.	1.1	14
48	CRT diagnosis of pulmonary disease: influence of monitor brightness and room illuminance on observer performance. Computerized Medical Imaging and Graphics, 2002, 26, 181-185.	3.5	13
49	A detection method for streak artifacts and radiological noise in a non-uniform region in a CT image. Physica Medica, 2010, 26, 157-165.	0.4	13
50	Information loss in visual assessments of medical images. European Journal of Radiology, 2007, 61, 362-366.	1.2	12
51	Influence of liquid crystal display monitors on observer performance for detection of diffuse pulmonary disease on chest radiographs. Radiation Medicine, 2007, 25, 211-217.	0.8	12
52	Method of measuring contrastâ€ŧoâ€noise ratio (<scp>CNR</scp>) in nonuniform image area in digital radiography. Electronics and Communications in Japan, 2013, 96, 32-41.	0.3	12
53	Renal sinus fat volume on computed tomography in middle-aged patients at risk for cardiovascular disease and its association with coronary artery calcification. Atherosclerosis, 2016, 246, 374-381.	0.4	12
54	Contrast enhancement efficacy of iodinated contrast media: Effect of molecular structure on contrast enhancement. European Journal of Radiology Open, 2018, 5, 183-188.	0.7	12

#	Article	IF	CITATIONS
55	Influence of Monitor Luminance Change on Observer Performance for Detection of Abnormalities Depicted on Chest Radiographs. Investigative Radiology, 2003, 38, 57-63.	3.5	11
56	Intraarterial cisplatin/nedaplatin and intravenous 5-fluorouracil with concurrent radiation therapy for patients with high-risk uterine cervical cancer. Gynecologic Oncology, 2006, 102, 493-499.	0.6	11
57	Sub-solid Nodule Detection Performance on Reduced-dose Computed Tomography with Iterative Reduction. Academic Radiology, 2017, 24, 995-1007.	1.3	11
58	Prediction of background parenchymal enhancement on breast MRI using mammography, ultrasonography, and diffusion-weighted imaging. Nagoya Journal of Medical Science, 2015, 77, 425-37.	0.6	11
59	A comparative contrast perception phantom image of brain CT study between high-grade and low-grade liquid crystal displays (LCDs) in electronic medical charts. Physica Medica, 2011, 27, 109-116.	0.4	10
60	Evaluation of a PC-based teleconferencing system for reading chest radiographs. Journal of Telemedicine and Telecare, 1999, 5, 122-125.	1.4	9
61	Fractal-Feature Distance Analysis of Radiographic Image. Academic Radiology, 2007, 14, 137-143.	1.3	9
62	Estimation of 123I-IMP Arterial Blood Activity Using 123I-IMP Acquisition Data From the Lungs and Brain Without Any Blood Sampling. Clinical Nuclear Medicine, 2012, 37, 258-263.	0.7	9
63	Images Acquired Using 320-MDCT With Adaptive Iterative Dose Reduction With Wide-Volume Acquisition: Visual Evaluation of Image Quality by 10 Radiologists Using an Abdominal Phantom. American Journal of Roentgenology, 2014, 202, 2-12.	1.0	9
64	Imaging of Endolymphatic Hydrops in 10 Minutes: A New Strategy to Reduce Scan Time to One Third. Magnetic Resonance in Medical Sciences, 2015, 14, 77-83.	1.1	9
65	Videotaped Helical CT Images for Lung Cancer Screening. Journal of Computer Assisted Tomography, 2000, 24, 242-246.	0.5	9
66	Use of an artificial neural network to differentiate between ECGs with IRBBB patterns of atrial septal defect and healthy subjects. Informatics for Health and Social Care, 2002, 27, 49-58.	1.0	8
67	Clinical outcomes of 125I brachytherapy with and without external-beam radiation therapy for localized prostate cancer: results from 300 patients at a single institution in Japan. Journal of Radiation Research, 2017, 58, 870-880.	0.8	8
68	Diagnostic usefulness of chest computed radiography—Film versus cathode-ray tube images. Journal of Digital Imaging, 1995, 8, 25-30.	1.6	7
69	Effects of monitor luminance change on observer detection performance. Computerized Medical Imaging and Graphics, 2005, 29, 35-41.	3.5	7
70	Influence of rib structure on detection of subtle lung nodules. European Journal of Radiology, 2006, 59, 49-55.	1.2	7
71	A new evaluation method for image noise reduction and usefulness of the spatially adaptive wavelet thresholding method for CT images. Australasian Physical and Engineering Sciences in Medicine, 2012, 35, 475-483.	1.4	7
72	Three-phase CT examination of the pancreatobiliary region using multislice CT with 1-mm collimation. Radiation Medicine, 2005, 23, 283-91.	0.8	7

5

#	Article	IF	CITATIONS
73	Widespread glucose hypometabolism in patients with hippocampal atrophy: Evaluation with 18F-fluorodeoxyglucose positron emission tomography. Journal of Epilepsy, 1997, 10, 155-160.	0.4	6
74	A phantom study for ground-glass nodule detectability using chest digital tomosynthesis with iterative reconstruction algorithm by ten observers: association with radiation dose and nodular characteristics. British Journal of Radiology, 2017, 90, 20160555.	1.0	6
75	StatSensor-i point-of-care creatinine analyzer may identify patients at high-risk of contrast-induced nephropathy. Experimental and Therapeutic Medicine, 2017, 13, 3503-3508.	0.8	6
76	Analysis of late adverse events and their chronological changes after radiation therapy for cervical cancer. Nagoya Journal of Medical Science, 2018, 80, 487-496.	0.6	6
77	The goal of PACS in Nagoya University Hospital. Computer Methods and Programs in Biomedicine, 1991, 36, 143-146.	2.6	4
78	Image storing system for radiation therapy (radiation oncology information system: ROIS) as a branch of diagnostic PACS; implementation and evaluation. Computerized Medical Imaging and Graphics, 1999, 23, 111-117.	3.5	4
79	The Application of Markov Theory to Contrast-Detail Analysis. Academic Radiology, 2006, 13, 152-158.	1.3	4
80	Fractal-feature distance as a substitute for observer performance index in contrast-detail examination. European Journal of Radiology, 2008, 67, 541-545.	1.2	4
81	Flat-Panel Detector Computed Tomography Imaging. Journal of Thoracic Imaging, 2012, 27, 51-57.	0.8	4
82	Development of distributed image database combined with clinical information in hospital information system. Journal of Medical Systems, 1995, 19, 305-311.	2.2	3
83	Estimation of the size of the media necessary to construct a medical image database. Computers in Biology and Medicine, 1996, 26, 77-85.	3.9	3
84	Interobserver agreement and performance score comparison in quality control using a breast phantom: screen-film mammography vs computed radiography. European Radiology, 2002, 12, 2192-2197.	2.3	3
85	Long-term Result of High Dose-rate Afterloading Brachytherapy in Squamous Cell Carcinoma of the Cervix: Relationship between Facility Structure and Outcome. Japanese Journal of Clinical Oncology, 2004, 34, 142-148.	0.6	3
86	A method of clustering observers with different visual characteristics. European Journal of Radiology, 2006, 57, 158-161.	1.2	3
87	Ultra-low-dose computed tomography system with a flat panel detector: assessment of radiation dose reduction and spatial and low contrast resolution. Radiation Medicine, 2008, 26, 627-635.	0.8	3
88	Quantitative assessment of the influence of anatomic noise on the detection of subtle lung nodule in digital chest radiography using fractal-feature distance. European Journal of Radiology, 2008, 68, 353-357.	1.2	3
89	A new automated assessment method for contrast–detail images by applying support vector machine and its robustness to nonlinear image processing. Australasian Physical and Engineering Sciences in Medicine, 2013, 36, 313-322.	1.4	3
90	Data set for renal sinus fat volume and visceral adipose tissue volume on computed tomography. Data in Brief, 2016, 7, 1658-1664.	0.5	3

#	Article	IF	CITATIONS
91	CSF Pulsation Artifacts on ADC Maps Obtained with Readout-segmented EPI. Magnetic Resonance in Medical Sciences, 2017, 16, 123-128.	1.1	3
92	RGSS-ID: An approach to new radiologic reporting system. Computerized Medical Imaging and Graphics, 1990, 14, 395-407.	3.5	2
93	Model analysis of time duration in a medication order entry system with attention to do-medication orders. Computers in Biology and Medicine, 1994, 24, 473-483.	3.9	2
94	A Signal-detection Experiment Measuring the Effect of Computer-aided Detection on Radiologists' Performance. Medical Decision Making, 2000, 20, 343-351.	1.2	2
95	A telemedicine system for collaborative work on radiographic coronary video-images. Journal of Telemedicine and Telecare, 2004, 10, 152-155.	1.4	2
96	Quantification of image quality using information theory. Australasian Physical and Engineering Sciences in Medicine, 2011, 34, 481-488.	1.4	2
97	Visualization of White Matter Tracts Using a Non-Diffusion Weighted Magnetic Resonance Imaging Method: Does Intravenous Gadolinium Injection Four Hours Prior to the Examination Affect the Visualization of White Matter Tracts?. PLoS ONE, 2014, 9, e91860.	1.1	2
98	Sub-solid nodule detectability in seven observers of seventy-nine clinical cases: comparison between ultra-low-dose chest digital tomosynthesis with iterative reconstruction and chest radiography by receiver-operating characteristics analysis. European Journal of Radiology, 2018, 107, 166-174.	1.2	2
99	Diagnostic Value of SPIO-mediated Breath-hold, Black-blood, Fluid-attenuated, Inversion Recovery (BH-BB-FLAIR) Imaging in Patients with Hepatocellular Carcinomas. Magnetic Resonance in Medical Sciences, 2010, 9, 49-58.	1.1	2
100	Is lower-dose digital fluorography diagnostically adequate compared with higher-dose digital radiography for the diagnosis of fallopian tube stenosis?. CardioVascular and Interventional Radiology, 2000, 23, 126-130.	0.9	1
101	Angiographic Guidewire with Measuring Markers: Design and Clinical Experience. CardioVascular and Interventional Radiology, 2006, 29, 981-985.	0.9	1
102	Three-Dimensional Intravenous Digital Subtraction Angiography Using Flat Panel Detector System in Vascular Mapping of the External Carotid Artery: A Comparison with 3-Dimensional Computed Tomography Angiography. Current Medical Imaging, 2009, 5, 216-221.	0.4	1
103	Ability of chest X-ray to detect faint shadows documented as ground-glass attenuation in images of computed tomography: A comparison between flat-panel detector radiography and film-screen radiography. European Journal of Radiology, 2010, 75, 384-390.	1.2	1
104	Effect of blue light from LCD on VDT work: Experiment using blue light reduction function LCD. Journal of the Society for Information Display, 2020, 28, 691-697.	0.8	1
105	Statistical method in a comparative study in which the standard treatment is superior to others. Nagoya Journal of Medical Science, 2002, 65, 127-32.	0.6	Ο